

Electron spin resonance observation of dehydration-induced spin excitations in quasi-one-dimensional iodo-bridged diplatinum complexes

Hisaaki Tanaka,^{1,*} Shin-ichi Kuroda,¹ Hiroaki Iguchi,² Shinya Takaishi,² and Masahiro Yamashita²

¹*Department of Applied Physics, Nagoya University, Furo-cho, Chikusa-ku, Nagoya 464-8603, Japan*

²*Graduate School of Science, Tohoku University, 6-3 Aza-Aoba, Aramaki, Sendai 980-8578, Japan*

(Received 1 December 2011; revised manuscript received 17 January 2012; published 21 February 2012)

Electron spin resonance (ESR) measurements have been performed on a series of quasi-one-dimensional iodo-bridged diplatinum complexes $K_2[C_3H_5R(NH_3)_2][Pt_2(pop)_4I] \cdot 4H_2O$ ($pop = P_2H_2O_5^{2-}$; $R = H, CH_3,$ or Cl), where dehydration/rehydration of the crystalline water switches the electronic state reversibly with retention of single crystallinity. We have observed a nonmagnetic nature in as-grown samples, whereas in the dehydrated samples, a clear enhancement of the spin susceptibility has been observed above ~ 80 K with the activation energy ranging 50–60 meV. The activated spins originate from isolated Pt^{3+} state on the chain, as confirmed from the principal g values. Concomitantly, the ESR linewidth exhibits a prominent motional narrowing, suggesting that the activated Pt^{3+} spins are mobile solitons generated in the doubly degenerate charge-density-wave states of the dehydrated salts.

DOI: [10.1103/PhysRevB.85.073104](https://doi.org/10.1103/PhysRevB.85.073104)

PACS number(s): 71.45.Lr, 76.30.He, 71.20.Rv

Quasi-one-dimensional (Q1D) halogen (X)-bridged metal (M) complexes, so-called MX -chains, have been extensively studied because they exhibit rich physical properties arising from their 1D charge-density-wave (CDW; $M = Pt$ or Pd) or Mott-Hubbard ($M = Ni$) ground states depending on the relative magnitude of electron-phonon or electron-electron interactions, respectively.^{1–4} In recent years, more sophisticated MMX -chain complexes have been attracting much interest.^{5–11} In these complexes, direct metal-metal bonding creates wider variety of valence-ordering states, typically represented as (a) averaged-valence (AV) state $[-M^{2.5+}-M^{2.5+}-X^- - M^{2.5+}-M^{2.5+}-X^-]$, (b) CDW state $[\cdots M^{2+}-M^{2+} \cdots X^- - M^{3+}-M^{3+}-X^- \cdots]$, (c) charge-polarization (CP) state $[\cdots M^{2+}-M^{3+}-X^- \cdots M^{2+}-M^{3+}-X^- \cdots]$, and (d) alternate-charge-polarization (ACP) state $[\cdots M^{2+}-M^{3+}-X^- - M^{3+}-M^{2+} \cdots X^- \cdots]$. The AV and the CP states have spin $S = 1/2$ on each metal dimer, whereas the CDW and the ACP states are doubly degenerate nonmagnetic states. In the CDW state the bridging halogen ions distort from the midpoint between the two $M-M$ units, whereas the dimerization of the $M-M$ units takes place in the ACP state, resulting in the two different $M-X-M$ bond lengths.

The MMX -chain compounds are categorized into two groups depending on the ligand molecule: a dithioacetate (dta) system, $M_2(RCS_2)_4I$ ($M = Ni, Pt$; $R =$ alkyl group),^{5,7,9,12,13} and a diphosphite (pop; $P_2H_2O_5^{2-}$) system, $A_4[Pt_2(pop)_4X] \cdot nH_2O$ or $A'_2[Pt_2(pop)_4X] \cdot nH_2O$ ($A =$ alkali metal, alkyl ammonium, etc.; $A' =$ alkyl diammonium; $X = Cl, Br, I$).^{6–8,14–16} The present study focuses on the latter system, the electronic state of which can be systematically controlled by replacing the countercations,^{8,14} removing crystalline water,^{15,16} or applying external pressure,¹⁴ etc. Iguchi *et al.* have recently synthesized a series of pop compounds which have binary countercations of potassium and propyldiammonium derivatives, $K_2[C_3H_5R(NH_3)_2][Pt_2(pop)_4I] \cdot 4H_2O$ ($R = H, CH_3,$ and Cl ; hereafter abbreviated as $NC_3N, Me-NC_3N,$ and $Cl-NC_3N$ salts, respectively).¹⁷ In these compounds a mixed valence-ordering state of ‘ACP + CDW’ $[(\cdots M^{2+}-M^{(2+\delta)+} \cdots X^- - M^{3+}-M^{(3-\delta)-}-X^- \cdots)]$, $0 < \delta < 1$ has been

suggested by x-ray structural analyses and polarized Raman spectra, i.e., two different values of Pt-I-Pt bond length ($d_{Pt-I-Pt}$) [shown in Fig. 1(a) for NC_3N salt], which is characteristic of the ACP state, and doublet structure of Pt-Pt stretching modes of Raman spectra, which is characteristic of the CDW state, have been observed.^{17,18} The ACP character in this salt is induced by the two types of coordination bonds between the $[Pt_2(pop)_4]$ units as shown by dashed lines in Fig. 1(a), which causes the two-fold periodic distortion of the units.

A pronounced feature in the case of NC_3N salt is that the crystalline water can be removed with retention of single crystallinity, which causes the following large change in structural and electronic properties.¹⁷ The ACP character disappears in the dehydrated salt, as shown in Fig. 1(b), resulting in a fairly small, single value of $d_{Pt-I-Pt}$ of 5.689(2) Å. The optical charge transfer energy (E_{CT}) decreases from 0.85 to 0.45 eV, which is the smallest value among all the pop compounds reflecting the small $d_{Pt-I-Pt}$, while it is still larger than that of $Pt_2(dta)_4I$ (0.3 eV) in the AV state.⁹ Although the halogen distortion characteristic of the CDW state has not been directly resolved by the x-ray structural analyses, the Raman spectrum exhibits a doublet structure, suggesting the CDW state for the dehydrated NC_3N salt. On the other hand, ³¹P MAS NMR spectrum exhibits a broadening by the dehydration at room temperature (RT), which indicates the presence of certain paramagnetic species. The spins are thermally activated as confirmed by our preliminary electron spin resonance (ESR) measurements for the polycrystalline samples,¹⁷ whereas the origin of these spins is still unclear because the CDW is a nonmagnetic state. In order to clarify the spin species, ESR spectroscopy provides the direct information through the principal g values, as demonstrated in the MX -^{3,19} and MMX -chain^{20–23} complexes. Furthermore, ESR linewidth and line shape provide dynamic information of spins in these systems.

In this Brief Report we performed detailed ESR measurements on NC_3N salt in order to clarify the magnetic properties before and after the dehydration, as well as the origin of the spin excitations reported in the dehydrated state. We used aligned single crystalline samples of NC_3N salt in order to obtain the

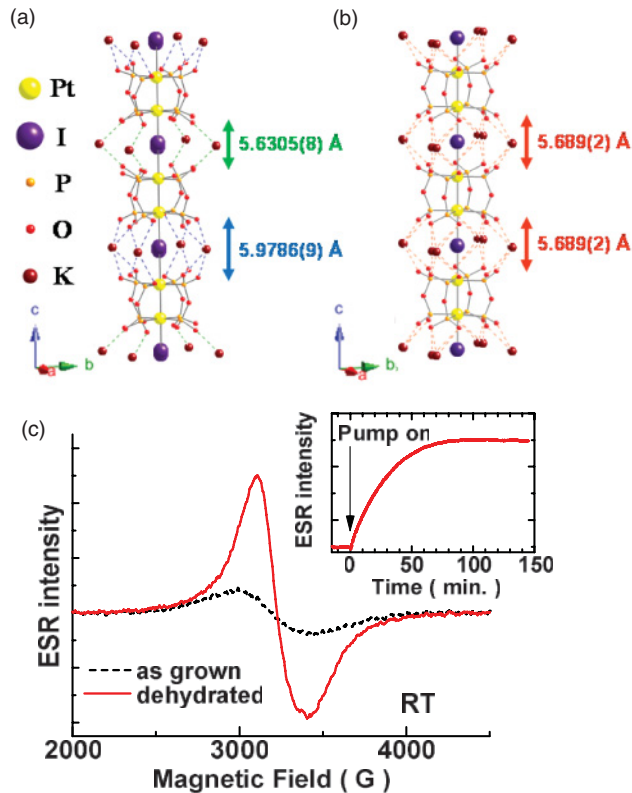


FIG. 1. (Color online) Crystal structures of NC_3N salt in (a) as-grown and (b) dehydrated states together with the Pt-I-Pt bond length ($d_{\text{Pt-I-Pt}}$).¹⁷ H atoms, H_2O molecules in (a) and $(\text{H}_3\text{NC}_3\text{H}_6\text{NH}_3)^{2+}$ ions are omitted for clarity. The dashed lines show the coordination bonds between potassium ions and oxygen atoms on the ligand. (c) First-derivative ESR spectra in as-grown (dashed curve) and dehydrated (solid curve) states of polycrystalline NC_3N salt at room temperature. The inset shows the time response of the ESR signal change by the vacuum treatment.

principal g values of dehydrated salts. In addition, we adopted Me- NC_3N and Cl- NC_3N salts, which can also be dehydrated, as in the case of NC_3N salt.¹⁷ We found a nonmagnetic nature in the as-grown samples with ‘ACP + CDW’ state and dehydrated samples below about 80 K of the CDW state. On the other hand, clear increase of the spin susceptibility was observed in all the dehydrated salts above 80 K. The origin of the spin was confirmed to be isolated Pt^{3+} state on the MMX -chain from the principal g values. Concomitantly, the ESR linewidth exhibited distinct motional narrowing above the same temperature range as the spin excitation took place, suggesting that the activated Pt^{3+} spins are mobile solitons generated in the doubly degenerated CDW state with small $d_{\text{Pt-I-Pt}}$.

Samples of NC_3N , Me- NC_3N , and Cl- NC_3N salts were prepared by the same methods as described elsewhere.^{17,18} In order to eliminate the water molecule of the as-grown samples, the samples were first evacuated at RT, and the change of the ESR signal was monitored. To complete the dehydration, the samples were heated up to 70 °C under the vacuum of 10^{-3} Pa. The single crystalline samples of NC_3N salt were used to determine the principal g values in the dehydrated state, whereas the ground polycrystalline samples were used

to obtain the spin susceptibility in order to avoid incomplete dehydration inside the bulky crystals. For Me- NC_3N and Cl- NC_3N salts, all the measurements were performed by using polycrystalline samples. ESR measurements were performed by using a Bruker EMX spectrometer at the X-band, as described previously.^{22,23}

Figure 1(c) shows the first-derivative ESR signals of as-grown (dashed curve) and dehydrated (solid curve) NC_3N polycrystalline samples at RT. The inset shows the time evolution of the ESR intensity with respect to the vacuum pumping at RT. We observe a clear enhancement of the ESR intensity in both figures by the dehydration of crystalline water. The water loss takes place by the evacuation at RT. In order to reveal the origin of the spin, we determined the principal g values from the single-crystal rotation measurements at RT. We observed the anisotropic g value of uniaxial type with the principal values of $g_{\parallel} = 1.966$ and $g_{\perp} = 2.147$ for the parallel and perpendicular directions to the chain, respectively, in the dehydrated state. Observed anisotropy of $g_{\perp} > 2 > g_{\parallel}$ is consistent with that expected for the low-spin Pt^{3+} ($S = 1/2$), where the unpaired electron resides on the $\text{Pt}(5d_z^2)$ orbital. Actually, the crystal-field calculation expects the principal g values of $g_{\perp} = 2 - 6(\lambda/\Delta) - 6(\lambda/\Delta)^2 > 2$ and $g_{\parallel} = 2 - 3(\lambda/\Delta)^2 < 2$, where Δ and λ denote the crystal-field splitting energy between d_z^2 and $d_{yz, zx}$ orbitals and spin-orbit coupling constant ($\lambda < 0$), respectively.²⁴ On the other hand, g_{\perp} value of the dehydrated state is smaller than those in the cases of the as-grown state of $g_{\perp} \sim 2.16 \pm 0.01$ at RT or Pt^{3+} in the dta-system of $g_{\perp} = 2.21$ typically,^{21–23} indicating the larger crystal-field splitting energy for the present dehydrated crystal due to the shorter Pt-I bond length. Similar anisotropy of the g value was observed with larger g_{\perp} value for the low-temperature Curie component, as will be mentioned using Fig. 3(a), indicating that the origin of the ESR signal is isolated Pt^{3+} state in the whole temperature region.

Figure 2 shows the temperature dependence of the first-derivative ESR signal of polycrystalline dehydrated NC_3N salts. We observe a broad Gaussian-like spectrum in the low temperature region, the linewidth of which may be partially originated from the hyperfine interaction with ^{195}Pt ($I = 1/2$) and ^{127}I ($I = 7/2$) nuclei, as in the case of ACP state in the dta system.^{21–23} However, the linewidth is nearly twice as broad in the present compounds than those in the dta system, indicating a contribution of dipolar interaction between the localized spins. A sharp signal marked by an asterisk (*) at 4 K arises from a small amount of extrinsic impurity, which becomes negligible at high temperatures. Above about 100 K, a clear narrowing of the linewidth is observed, resulting in a Lorentzian-like spectrum in the high temperature region. Similar temperature dependence of the linewidth and line shape was also observed in the dehydrated states of other two salts: Me- NC_3N and Cl- NC_3N . As will be discussed by using Figs. 3(a) and 3(b) below, the narrowing takes place in the same temperature range where the spin susceptibility exhibits activation-type increase. The observed narrowing strongly indicates the occurrence of motional narrowing due to the thermal motion of the activated spins, which is likely to be spin solitons. Although the motional narrowing in the pure 1D system provides non-Lorentzian line shape due to the so-called long time tail of the spin-correlation function, finite interchain

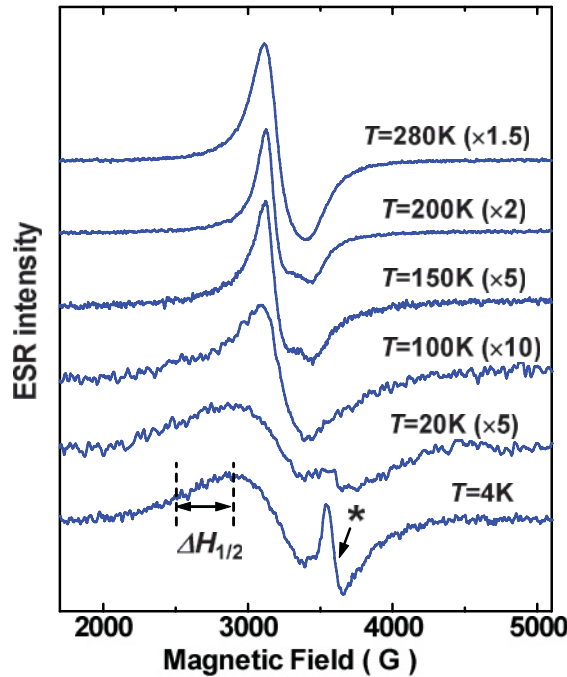


FIG. 2. (Color online) Temperature dependence of the first-derivative ESR spectrum of dehydrated NC_3N salt (polycrystalline samples).

hopping causes the cut off of this lasting tail to provide a Lorentzian line shape,²⁵ which is also the case of ESR signal of Q1D conduction electrons or thermally activated solitons in the dta compound.²² On further heating, the linewidth starts to increase above 200 K, as shown in Figs. 2 and 3(b), probably due to the shortening of the spin-lattice relaxation time for high temperatures.

Figure 3 shows the temperature dependence of (a) spin susceptibility χ and (b) ESR linewidth $\Delta H_{1/2}$, obtained for as grown (open circles) and dehydrated (solid circles) samples of NC_3N salt. The linewidth is defined as the width of the lower-field side of the upper peak of the first-derivative ESR signal at half maximum, as defined in Fig. 2. Thus defined linewidth is unaffected by the unresolved g anisotropy, which causes the additional line broadening in the case of conventional peak-to-peak linewidth in the polycrystalline samples. In the as-grown samples, χ obeys the Curie law in the whole temperature region, as shown by the dashed curve, with the spin concentration of 1 spin per 10^3 MMX units. The origin of the Curie component may be ascribed to the free spins at the structural defects such as chain ends.¹⁹ The result indicates that the ‘ACP + CDW’ state in as-grown samples is nonmagnetic, as expected. On the other hand, χ exhibits a clearly different temperature dependence in the dehydrated salts; it obeys the Curie law at low temperature region with markedly lower spin concentration of 1 spin per 5×10^3 MMX units, whereas it exhibits a remarkable increase from the Curie law above about 80 K. As for the ESR linewidth, it exhibits a clear narrowing above the same temperature range as shown in (b), which is not the case for the as grown samples.

The small spin susceptibility below 80 K indicates that the ground state of the dehydrated sample is nonmagnetic, which is consistent with the Raman experiments expecting the CDW

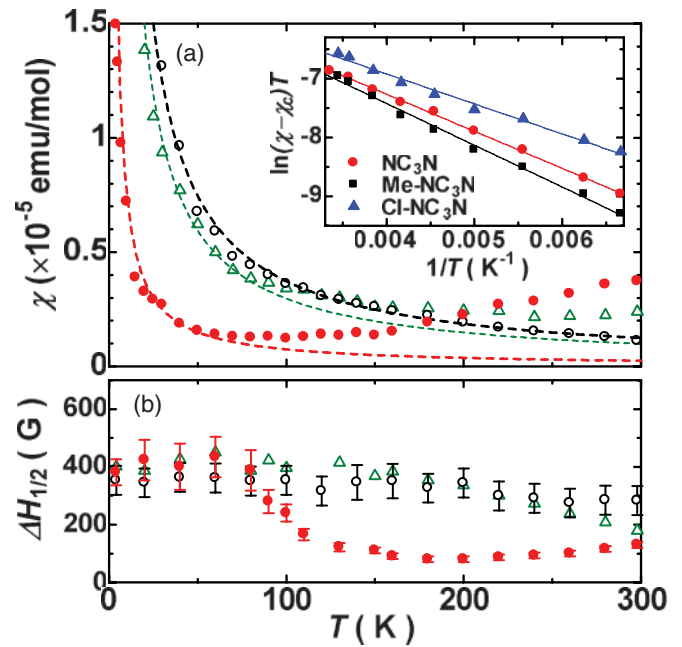


FIG. 3. (Color online) Temperature dependence of (a) spin susceptibility (χ) and (b) ESR linewidth ($\Delta H_{1/2}$) obtained for the as-grown (open circles), dehydrated (solid circles), and rehydrated (open triangles) samples of NC_3N salt. The dashed curves in (a) represent the fitting by the Curie law. The inset in (a) shows the plot of $\Delta\chi \cdot T$ versus inverse temperature obtained for the three dehydrated salts of NC_3N (circles), $\text{Me-NC}_3\text{N}$ (rectangles), and $\text{Cl-NC}_3\text{N}$ (triangles). The solid lines show the fitting by the activation formula.

state. In addition, the decrease of Curie-spin concentration in the dehydrated samples indicates that dehydration produces no defects, which is consistent with the high crystallinity reported in the dehydrated salts.¹⁷ The observed decrease may be, for example, caused by the formation of a singlet state between the adjacent localized spins at the defect sites due to the larger overlap of the wave functions, reflecting the shortening of $d_{\text{Pt-I-Pt}}$ in the dehydrated salts. On the other hand, the increase of χ above 80 K, shown in Fig. 3(a), indicates the activation of paramagnetic Pt^{3+} spins. The enhanced component $\Delta\chi$ ($\equiv \chi - \chi_C$) is well fitted by the activation-type formula, $\Delta\chi \cdot T = C \exp(-E_g/k_B T)$, as shown in the inset. Here, χ_C is Curie spin susceptibility, C is the Curie constant for the activated spins, and k_B is the Boltzmann constant. Similar temperature dependence of χ has been observed in all the dehydrated compounds used in this study, and the results of $\Delta\chi$ are also shown in the inset. Estimated activation energy E_g ranges 50–60 meV in these salts, and the activated spin concentration is about 1 spin per 300–400 MMX units at RT, which is an order of magnitude larger than that of the Curie component.

Interestingly, both the spin susceptibility and ESR linewidth returns to almost initial behavior of the as-grown salt by exposing the dehydrated salt to the H_2O vapor for several days at RT, as shown by the open triangles in Fig. 3. This clearly indicates that the dehydration/rehydration takes place reversibly, consistent with the x-ray analyses,¹⁷ although the rehydration is not perfect in the present experimental condition and a finite contribution of activated spin is observed for high temperatures.

As pointed out previously, the activation of the Pt^{3+} spin in the dehydrated salt is associated with the narrowing of the ESR signal due to the thermal motion of the spins (motional narrowing). Despite the coexistence of the Curie and activated spins at high temperatures, spin motion allows them to approach each other, resulting in the exchange-coupled single ESR line.^{21,22} Obviously, the dominant contribution to the ESR signal is an activated component at high temperature region. Such activated mobile spins in the CDW state are regarded as soliton-kink in the CDW state, that is, isolated Pt^{3+} state (or $[\text{Pt}^{2+}-\text{Pt}^{3+}]$ unit) locating at the mismatch of the doubly degenerate valence-ordering phases of $[\dots\text{Pt}^{2+}-\text{Pt}^{2+}\dots\text{I}^- - \text{Pt}^{3+}-\text{Pt}^{3+}-\text{I}^- \dots]$ and $[-\text{Pt}^{3+}-\text{Pt}^{3+}-\text{I}^- \dots\text{Pt}^{2+}-\text{Pt}^{2+}\dots\text{I}^-]$. The formation of solitons has been predicted theoretically in the case of CDW and ACP states in the *MMX*-chain compounds by using Peierls-Hubbard model²⁶⁻²⁸ and has been actually demonstrated in the case of the ACP state of a dta compound $\text{Pt}_2(n\text{-pentyICS}_2)_4\text{I}$ by the ESR technique.^{21,22} On the other hand, there has been no report of thermally activated solitons in the pop compounds by the reason pointed out subsequently.

When the amplitude of the CDW, or the halogen distortion, in other words, becomes small, the soliton can be easily created by the thermal energy, as is the case of the *MX*-chain complex having Pd-Br chain.³ In the case of the CDW in pop compounds, $d_{\text{Pt-I-Pt}}$ is a good measure for the amplitude of the CDW; smaller $d_{\text{Pt-I-Pt}}$ results in the smaller amplitude of the CDW, as reflected on the decrease of the optical gap energy.¹⁴ The pop compounds examined so far have relatively large $d_{\text{Pt-I-Pt}}$,^{14,20} and then, the phase mismatch of the CDW state is hardly created. In the dehydrated NC_3N salt, on the other hand, halogen distortion is very small due to small $d_{\text{Pt-I-Pt}}$, and the x-ray structural analyses cannot resolve the distortion.¹⁷ As for the $\text{Me-NC}_3\text{N}$ and $\text{Cl-NC}_3\text{N}$ salts, $d_{\text{Pt-I-Pt}}$ has not been determined for the dehydrated samples. However,

lattice constant of the *c*-axis (chain axis) determined by the powder x-ray diffraction measurements decreases in the order 8.487 \AA (NC_3N) $>$ 8.470 \AA ($\text{Cl-NC}_3\text{N}$) $>$ 8.467 \AA ($\text{Me-NC}_3\text{N}$),¹⁷ implying that $d_{\text{Pt-I-Pt}}$ in these dehydrated salts takes no larger values than that in the dehydrated NC_3N salt. This small $d_{\text{Pt-I-Pt}}$ value in the dehydrated state may be the reason for the thermal activation of solitons in these three compounds.

We point out here that the activation energy of the soliton excitation in the present pop compounds is still larger than that determined in $\text{Pt}_2(n\text{-pentyICS}_2)_4\text{I}$ of less than 10 meV.^{21,22} This may indicate that the lattice deformation energy is larger than that in the ACP state of the dta compound. In this context, application of high pressure in the present dehydrated salts is an interesting subject to reduce the generation energy of the soliton. Furthermore, when $d_{\text{Pt-I-Pt}}$ becomes sufficiently small, the system is expected to undergo the phase transition into the AV state or even a metallic state.^{10,11} Experimental observation of such transition is left open for future studies.

In summary, present ESR measurements on the three pop compounds have revealed that the crystalline water modulates the magnetic properties remarkably through the change of Pt-I bond length. Although the ground state of the dehydrated crystals is nonmagnetic, which is consistent with the CDW state suggested by Raman results, thermal activation of Pt^{3+} spins causes clear enhancement of the spin susceptibility at RT, which is consistent with the broadening of the NMR spectrum. The motional narrowing of the ESR signal suggests that the activated Pt^{3+} spins are mobile solitons in the doubly degenerate CDW state.

This work has been partially supported by Grant-in-Aid for Scientific Research (Grants No. 21740224 and No. 22340080) from the Ministry of Education Culture, Sports, Science and Technology of Japan.

*htanaka@nuap.nagoya-u.ac.jp

¹P. Day, in *Low Dimensional Cooperative Phenomena*, edited by H. J. Keller (Plenum Press, New York, 1974).

²H. Okamoto and M. Yamashita, *Bull. Chem. Soc. Jpn.* **71**, 2023 (1998), and references therein.

³H. Okamoto, K. Toriumi, T. Mitani, and M. Yamashita, *Phys. Rev. B* **42**, 10381 (1990).

⁴H. Kishida, H. Matsuzaki, H. Okamoto, T. Manabe, M. Yamashita, T. Taguchi, and Y. Tokura, *Nature* **405**, 929 (2000).

⁵C. Bellitto, A. Flamini, L. Gastaldi, and L. Scaramuzza, *Inorg. Chem.* **22**, 444 (1983).

⁶C.-M. Che, F. H. Herbstein, W. P. Schaefer, R. E. Marsch, and H. B. Gray, *J. Am. Chem. Soc.* **105**, 4604 (1983).

⁷M. Yamashita, S. Takaishi, A. Kobayashi, H. Kitagawa, H. Matsuzaki, and H. Okamoto, *Coord. Chem. Rev.* **250**, 2335 (2006).

⁸M. Yamashita, S. Miya, T. Kawashima, T. Manabe, T. Sonoyama, H. Kitagawa, T. Mitani, H. Okamoto, and R. Ikeda, *J. Am. Chem. Soc.* **121**, 2321 (1999).

⁹H. Kitagawa, N. Onodera, T. Sonoyama, M. Yamamoto, M. Fukawa, T. Mitani, M. Seto, and Y. Maeda, *J. Am. Chem. Soc.* **121**, 10068 (1999).

¹⁰S. Yamamoto, *Phys. Rev. B* **64**, 140102 (2001).

¹¹M. Kuwabara and K. Yonemitsu, *J. Mater. Chem.* **11**, 2163 (2001).

¹²M. Mitsumi, T. Murase, H. Kishida, T. Yoshinari, Y. Ozawa, K. Toriumi, T. Sonoyama, H. Kitagawa, and T. Mitani, *J. Am. Chem. Soc.* **123**, 11179 (2001).

¹³M. Mitsumi, K. Kitamura, A. Morinaga, Y. Ozawa, M. Kobayashi, K. Toriumi, Y. Iso, H. Kitagawa, and T. Mitani, *Angew. Chem. Int. Ed.* **41**, 2767 (2002).

¹⁴H. Matsuzaki, T. Matsuoka, H. Kishida, K. Takizawa, H. Miyasaka, K. Sugiura, M. Yamashita, and H. Okamoto, *Phys. Rev. Lett.* **90**, 046401 (2003).

¹⁵H. Matsuzaki, H. Kishida, H. Okamoto, K. Takizawa, S. Matsunaga, S. Takaishi, H. Miyasaka, K. Sugiura, and M. Yamasita, *Angew. Chem. Int. Ed.* **44**, 3240 (2005).

¹⁶H. Iguchi, S. Takaishi, T. Kajiwara, H. Miyasaka, M. Yamashita, H. Matsuzaki, and H. Okamoto, *J. Inorg. Organomet. Polym. Mater.* **19**, 85 (2009).

¹⁷H. Iguchi, S. Takaishi, H. Miyasaka, M. Yamashita, H. Matsuzaki, H. Okamoto, H. Tanaka, and S. Kuroda, *Angew. Chem. Int. Ed.* **49**, 552 (2010).

- ¹⁸H. Iguchi, S. Takaishi, T. Kajiwara, H. Miyasaka, M. Yamashita, H. Matsuzaki, and H. Okamoto, *J. Am. Chem. Soc.* **130**, 17668 (2008).
- ¹⁹K. Marumoto, H. Tanaka, S. Kuroda, T. Manabe, and M. Yamashita, *Phys. Rev. B* **60**, 7699 (1999).
- ²⁰K. Marumoto, H. Tanaka, S. Kozaki, S. I. Kuroda, S. Miya, T. Kawashima, and M. Yamashita, *Solid State Commun.* **120**, 101 (2001).
- ²¹H. Tanaka, S. I. Kuroda, T. Yamashita, M. Mitsumi, and K. Toriumi, *J. Phys. Soc. Jpn.* **72**, 2169 (2003).
- ²²H. Tanaka, S. I. Kuroda, T. Yamashita, M. Mitsumi, and K. Toriumi, *Phys. Rev. B* **73**, 245102 (2006).
- ²³H. Tanaka, H. Nishiyama, S. I. Kuroda, T. Yamashita, M. Mitsumi, and K. Toriumi, *Phys. Rev. B* **78**, 033104 (2008).
- ²⁴J. M. Assour, *J. Chem. Phys.* **43**, 2477 (1965).
- ²⁵M. J. Hennessy, C. D. McElwee, and P. M. Richards, *Phys. Rev. B* **7**, 930 (1973).
- ²⁶S. Yamamoto and M. Ichioka, *J. Phys. Soc. Jpn.* **71**, 189 (2002).
- ²⁷J. Ohara and S. Yamamoto, *Phys. Rev. B* **73**, 045122 (2006).
- ²⁸M. Kuwabara, K. Yonemitsu, and H. Ohta, in *EPR in the 21st Century*, edited by A. Kawamori, J. Yamaguchi, and H. Ohta (Elsevier Science, 2002), p. 59.